

Cell elasticity measurement using a microfluidic device with real-time pressure feedback

Zhenlin Chen^a, Yonggang Zhu^a, Dong Xu^a, Md. Mahbub Alam^a, Lingling Shui^b and Huaying Chen^{a*}

^a School of Mechanical Engineering and Automation, Harbin Institute of Technology, Shenzhen, Shenzhen 518055, China.

^b School of Information and Optoelectronic Science and Engineering, South China Normal University, China

* Corresponding Author

KEYWORDS:

ABSTRACT: The study of cell elasticity provides new insights into not only cell biology but also disease diagnosis based on cell mechanical state variation. Microfluidic technologies have made noticeable progress in studying cell deformation with the capabilities of high throughput and automation. This paper reports the development of a novel microfluidic system to precisely measure elasticity of cells having large deformation in a constriction channel. It integrated i) a separation unit to isolated- or flake-shaped particles that might block the constriction channel to increase the measurement throughput and ii) a pressure feedback system precisely detecting the pressure drop inducing the deformation of each cell. The fluid dynamics of the separation unit was modeled to understand the separation mechanism before the experimental determination of separation efficiency. Afterward, the pressure system was characterized to demonstrate its sensitivity and reproducibility in measuring the subtle pressure drop along a constriction channel. Finally, the microfluidic system was employed to study the stiffness of both K562 and endothelial cells. The cell protrusion and pressure drop were employed to calculate the mechanical properties based on a power-law rheology model describing the viscoelastic behaviors of cells. Both the stiffness and the fluidity of K562 cells were consistent with previous studies. The system is of remarkable application potential in the precise evaluation of cell mechanical properties.

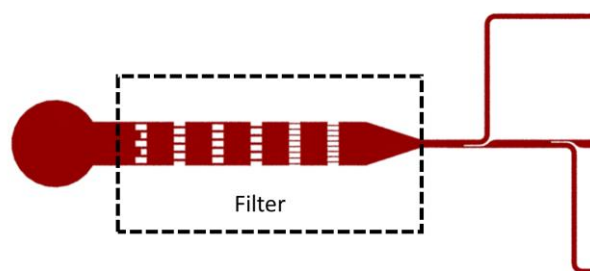


Figure S1. The multi-level filtration unit.

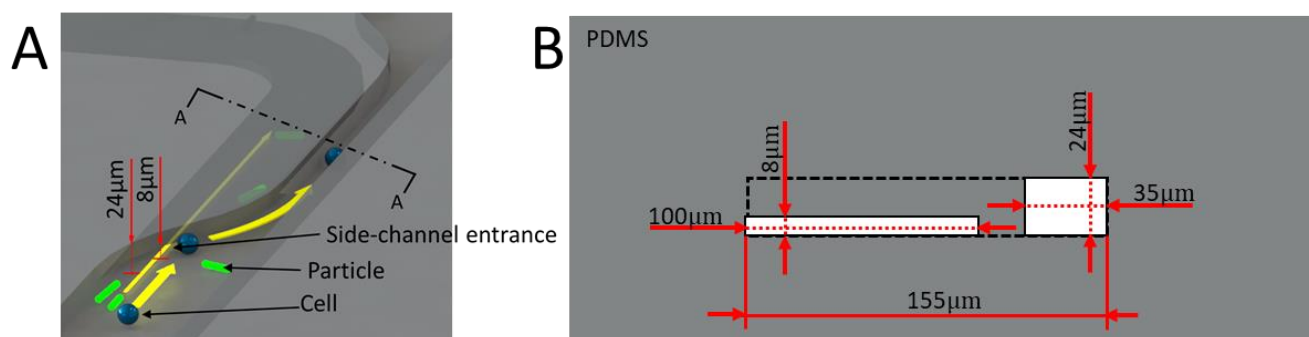


Figure S2. (A) An inset of the side channel entrance in the separation unit. (B) The dimension of the cross-section through line A-A.

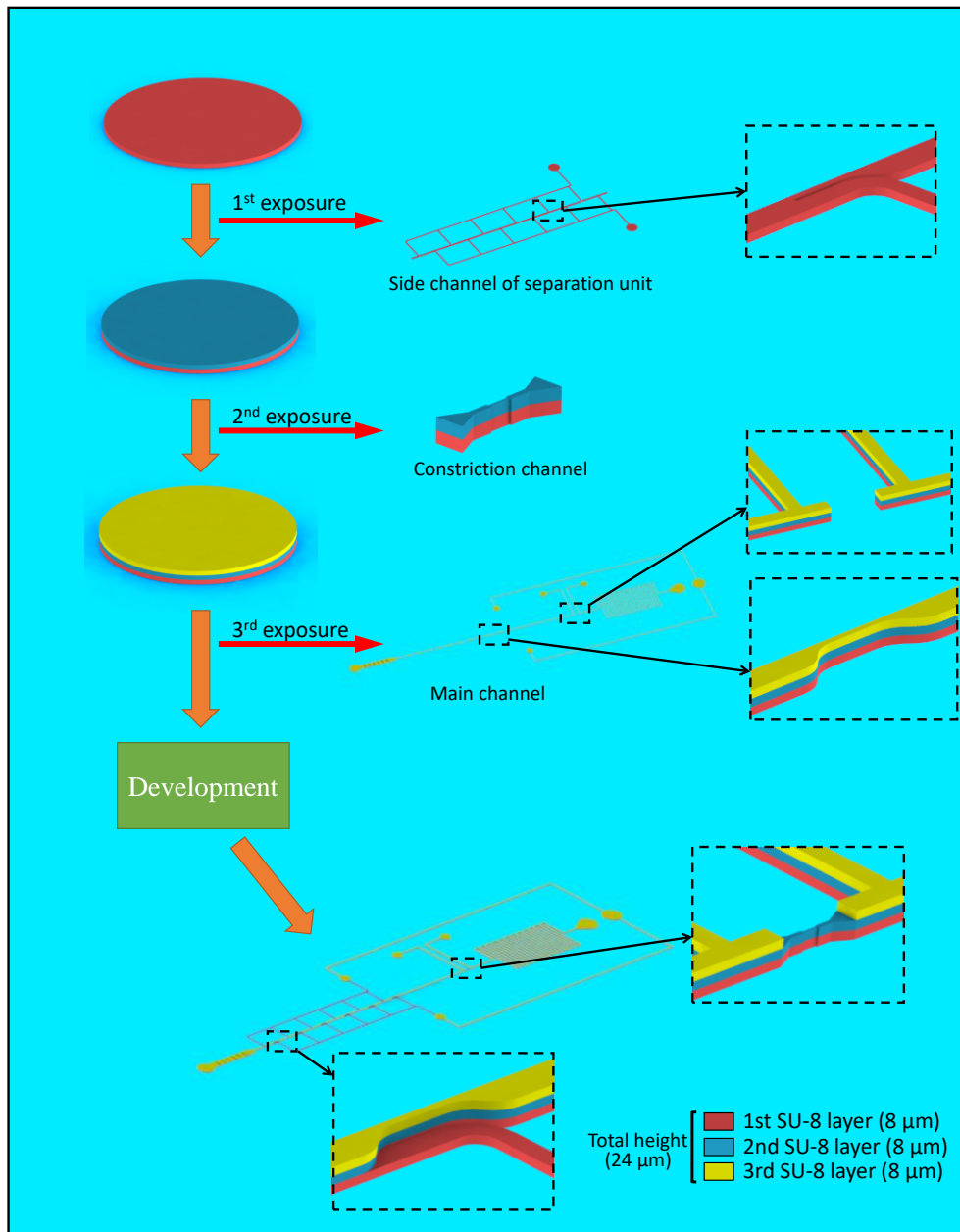


Figure S3. The multiple-lithography process for the manufacture of the SU-8 mold for the microfluidic chip. Following 30 minute dehydration at 200 °C, the wafer was spin-coated with SU-8 2007 (MicroChem, Newton, MA, USA) at 1800 rpm to obtain an 8-μm thick film. It was then baked at 95 °C for 4 minutes. Afterward, it was exposed to UV light (URE-2000, Chinese Academy of Sciences, Beijing, China) with a dose of 120 mJ/cm² under a photomask with the separation unit (The 1st exposure) before baked at 65 °C for 3 minutes. After the second SU-8 layer was spin coated and baked, the pattern for the constriction channel was exposed to UV light (The 1st exposure) with the same dose as above. After the post exposure bake at 65 for 3 minutes, the third SU-8 layer was fabricated. Then the photoresist was exposed to UV light under the pattern (The 3rd exposure).

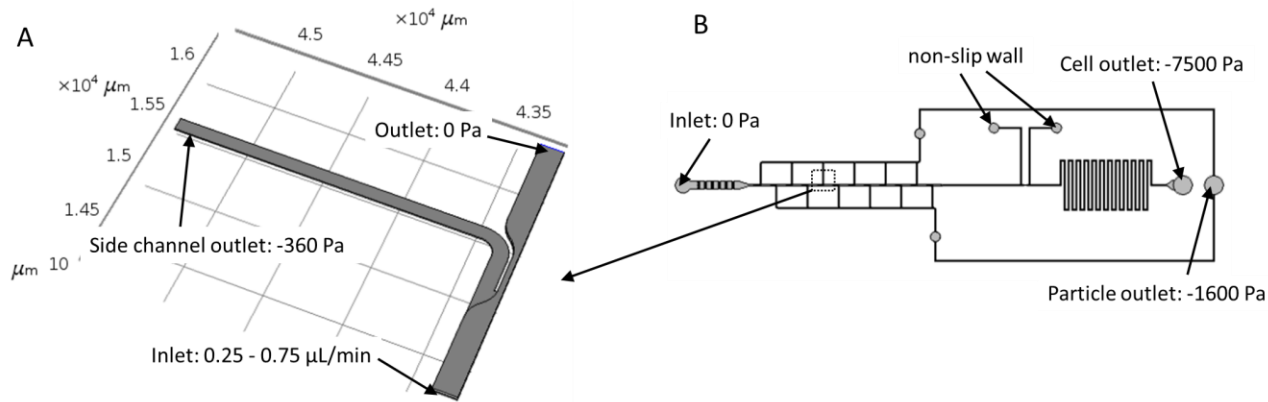


Figure S4. (A) The simplified model of one level of the separation unit to study fluid dynamics in Section 2.2. (B) The whole device used in the simulation to figure out the pressure (-360 Pa) for the outlet port of the model in figure A. The pressure at the inlet, cell outlet, and particle outlet ports used in the simulation and the experiment was listed in figure B. To reduce the computation time, all the simulation about the separation unit was performed using the model in Figure S4A. Since we only modeled the flow distribution, it is reasonable to employ Figure S4A to simplify the whole device.

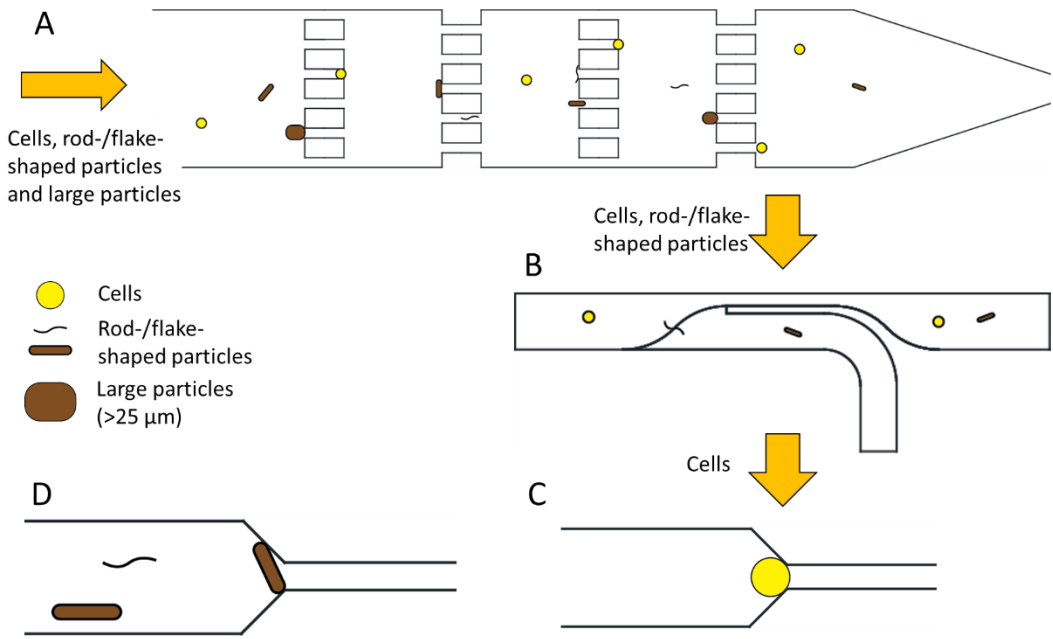


Figure S5 Schematic of the particle separation and channel blockage. (A) The multi-level separate large particles (>25 μm); (B) The separation unit isolate rod-/flake-shaped particles to the side channels; (C) Only cells reach the contraction channel; (D) Rod-/flake-shaped particles may block the contraction channel due to the sudden change of the flow stream at the entrance of the constriction channel.

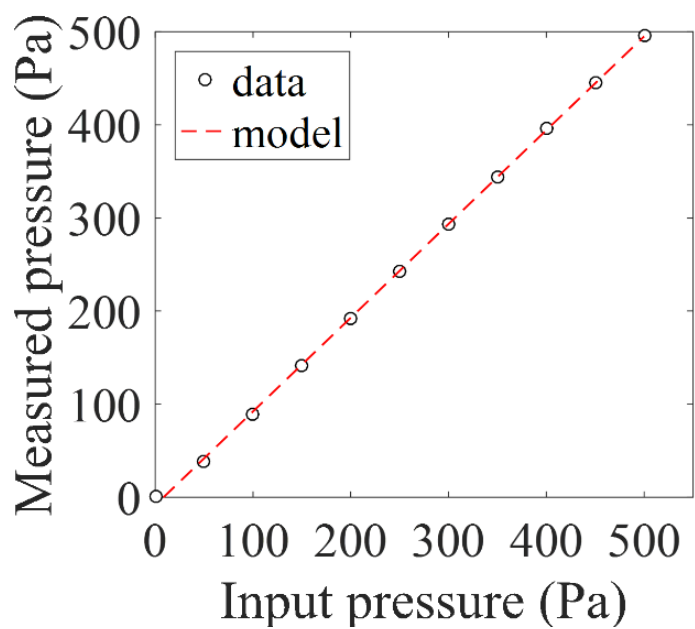


Figure S6. The relationship between pressure measured by the DPS and the input pressure. The line represents the model of $y=1.007x-8.563$ ($R^2 = 0.999$).

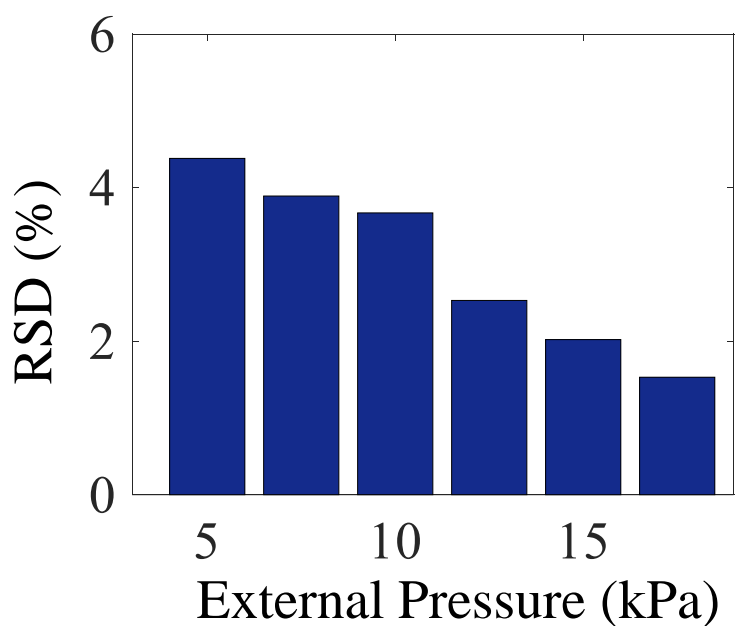


Figure S7. The relative standard deviation (RSD) when the measured pressure drop along the constriction channel (without cells) was measured using the pressure feedback system.

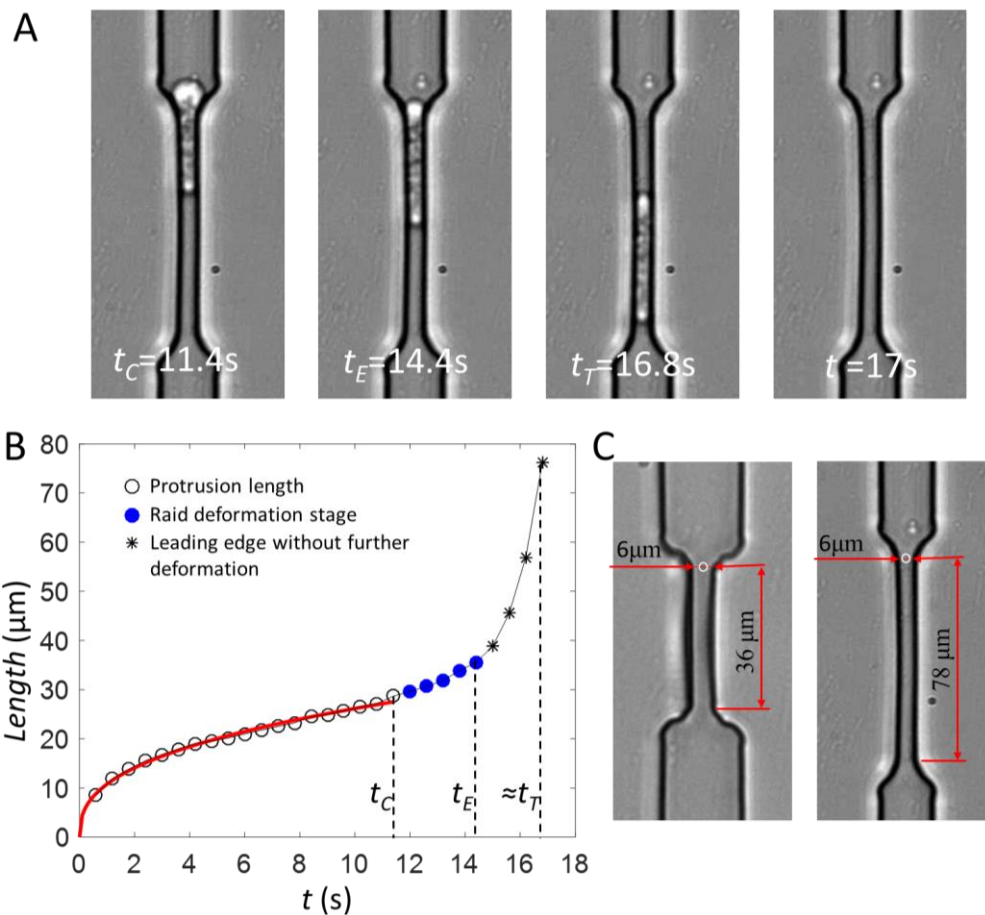


Figure S8. (A) The micro photos of the K562 cell images at different times points. (B) The deformation and traveling of a K562 cell in a $78\mu\text{m}$ long constriction channel. Hollow circles were employed to fit the power-law rheology model. The filled circles represented the rapid increase stage of the deformation. The creep time (t_C) is the period for fitting the power-law rheology model. The entry time (t_E) is defined as the period from the beginning to the end of the cell deformation. The transit time (t_T) is the period for the whole cell to pass through the constriction channel. (C) The actual length of the constriction channel. The constriction channel with the width of $6\mu\text{m}$, and the origins (white circles) of cell protrusion length measurement.

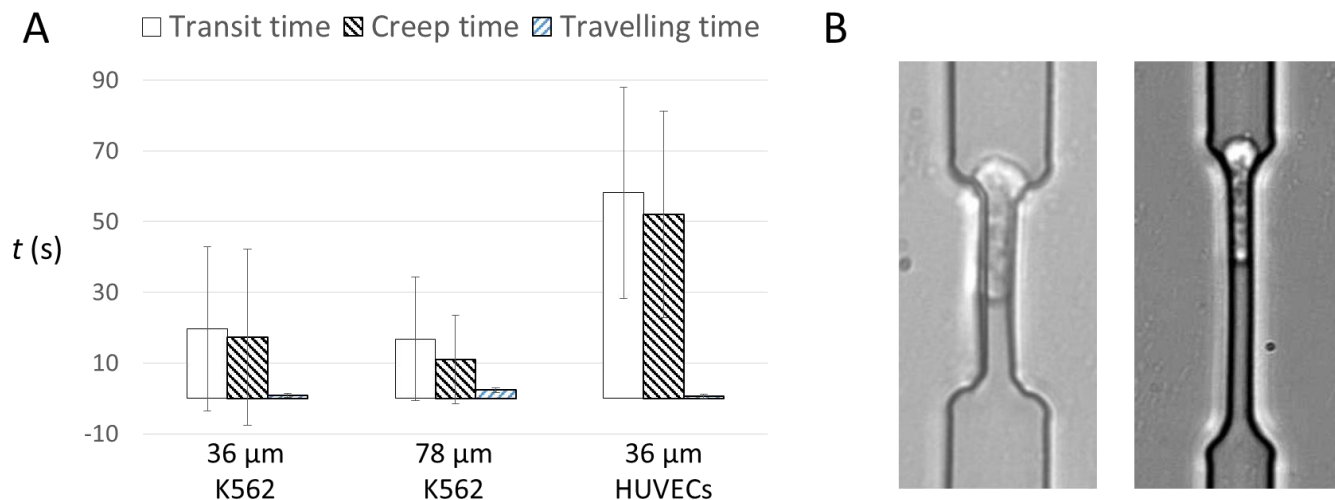


Figure S9. (A) The transit time, creep time and traveling time of K562 cells and HUVECs in constriction channels with different lengths. (B) The micro photos showing the rest length for cells to travel in the 36 μm (left) and 78 μm (right) channels.

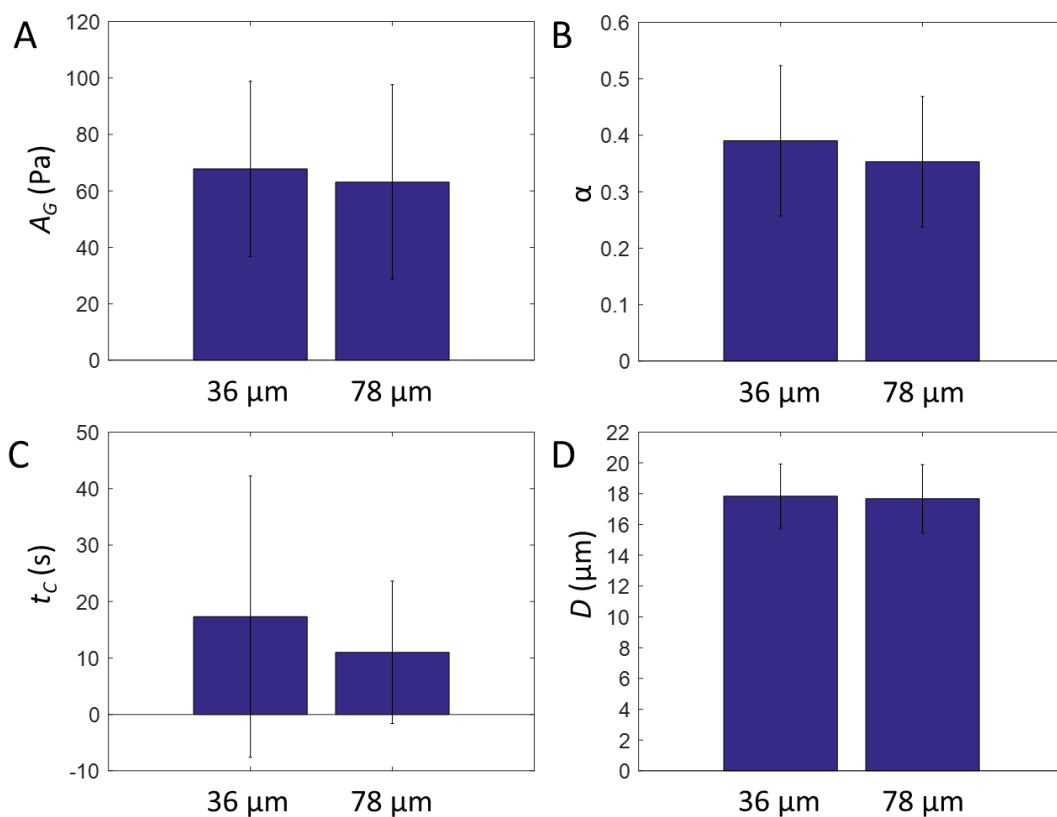


Figure S10. (A) The stiffness constant (A_G), (B) power-law exponent (α), (C) creep time (t_c) and (D) cell diameter (D) for cells passing through the 36 μm and 78 μm constriction channels.

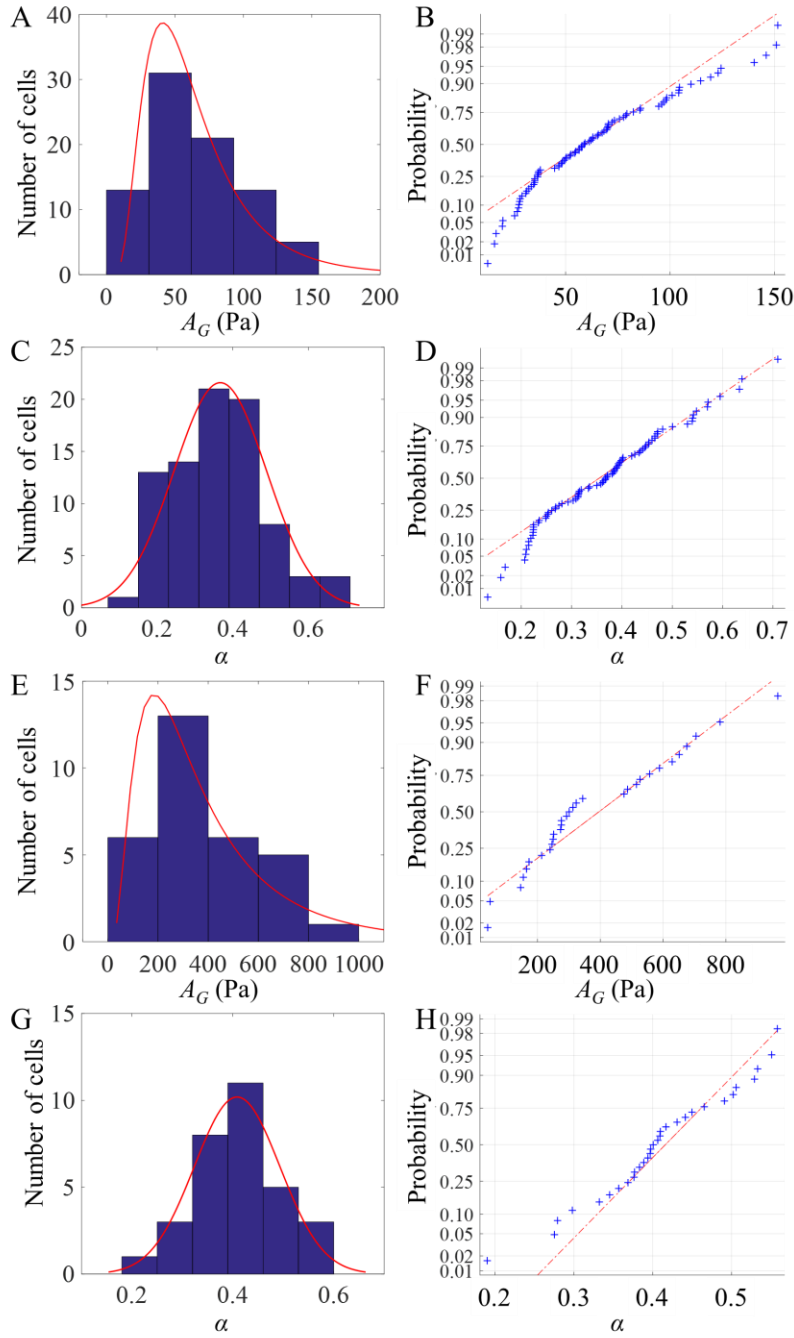
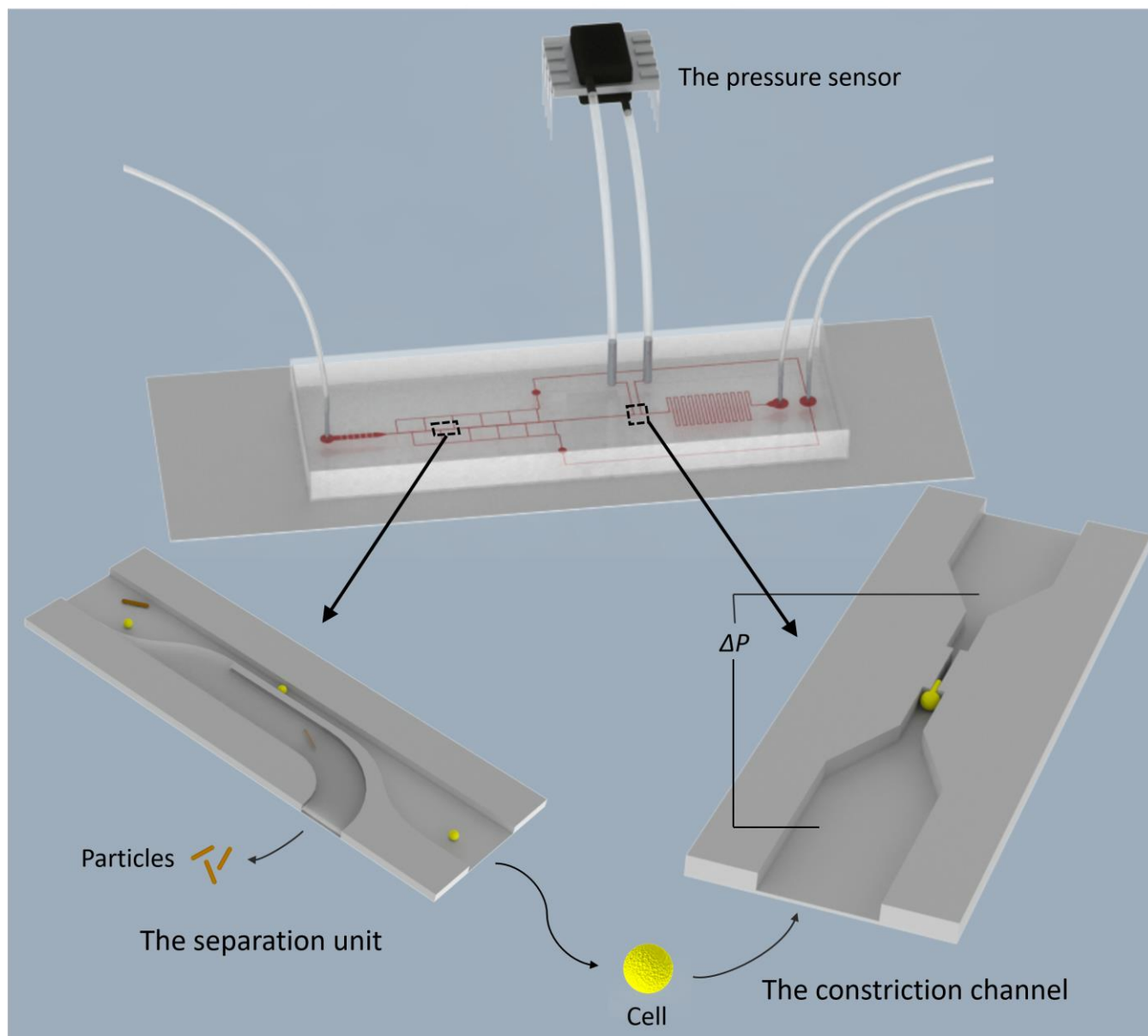


Figure S11. The lognormal distribution and relevant probability plots of cell stiffness of K562 cells (A and B) and HUVECs (E and F) with p values of 0.58 and 0.15, respectively. The distribution and relevant normal probability plots of power-law exponents of K562 cells (C and D) and HUVECs (G and H), with p values of 0.48 and 0.51, respectively. The Lilliefors test was employed for the analysis of both distributions.



A microfluidic system integrating a separation unit and a pressure sensor to accurately measure cell elasticity.